Supporting information

Sb_2Te_3 topological insulator: surface plasmon resonance and application in refractive index monitoring

Hua Lu, *[a] Siqing Dai,[a] Zengji Yue,[b] Yicun Fan,[a] Huachao Cheng,[a] Jianglei Di,[a] Dong Mao,[a] Enpu Li,[a] Ting Mei[a] and Jianlin Zhao*[a]

[a]*MOE Key Laboratory of Material Physics and Chemistry under Extraordinary Conditions, and Shaanxi Key Laboratory of Optical Information Technology, School of Science, Northwestern Polytechnical University, Xi'an 710072, China*

[b]*Institute for Superconducting & Electronic Materials, University of Wollongong, North Wollongong, New South Wales 2500, Australia*

*E-mail: hualu@nwpu.edu.cn; jlzhao@nwpu.edu.cn

Contents

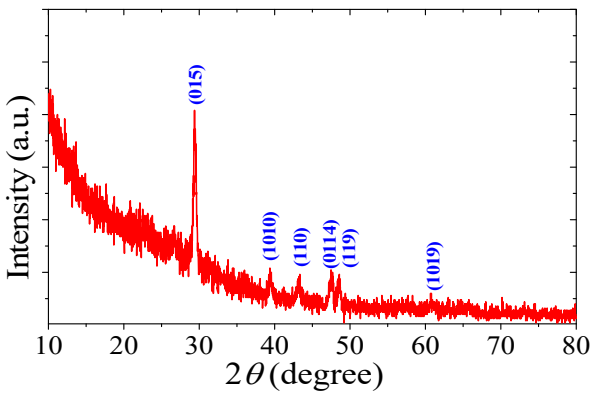

Figure S1. XRD patterns of the Sb_2Te_3 material.

Dielectric constants of the Sb_2Te_3 material

According to the Tauc-Lorentz model, the imaginary part ε_b'' of the dielectric function for the semiconductor bulk layer of the Sb_2Te_3 material can be given by [1]

$$\varepsilon_b''(E)=\begin{cases}\dfrac{AE_0C(E-E_g)^2}{(E^2-E_0^2)^2+C^2E^2}\cdot\dfrac{1}{E}, & (E>E_g)\\ 0 & (E\le E_g)\end{cases} \tag{1}$$

The real part ε_b' of the dielectric function for the semiconductor bulk layer can be achieved by Kramers-Kronig integration, which is described as

$$\varepsilon_b'(E)=\varepsilon_b''(\infty)+\frac{2}{\pi}P\int_{E_g}^{\infty}\frac{\xi\varepsilon_b''(\xi)}{\xi^2-E^2}d\xi, \tag{2}$$

where A, E_0, C, E_g, and $\varepsilon_1(\infty)$ are the fitting parameters corresponding to the amplitude of absorption peak, peak in joint density of states, broadening factor, band gap and high frequency dielectric constant, respectively. E stands for the photon energy, and P represents the Cauchy principal part of the integral. These parameters are fitted as A=111.677, E_0=1.910 eV, C=2.604, E_g=0.282 eV, and $\varepsilon_1(\infty)$=2.353. The dielectric constant of the metal-like surface layer can be fitted by the Drude model,[2]

$$\varepsilon_s(\omega)=\varepsilon_\infty-\frac{\omega_p^2}{\omega(\omega+i\gamma)}, \tag{3}$$

where ε_∞, γ, and ω_p are the dielectric constant at the infinite frequency, electron collision frequency and bulk plasma frequency, respectively. The parameters are fitted as ε_∞=7.099, ω_p=13.160 eV and γ=0.355 eV. ω stands for the angular frequency in vacuum.

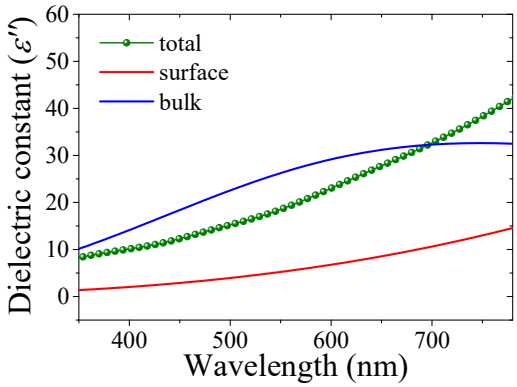

Figure S2. Imaginary parts of dielectric constants of the Sb_2Te_3 material in the visible region.

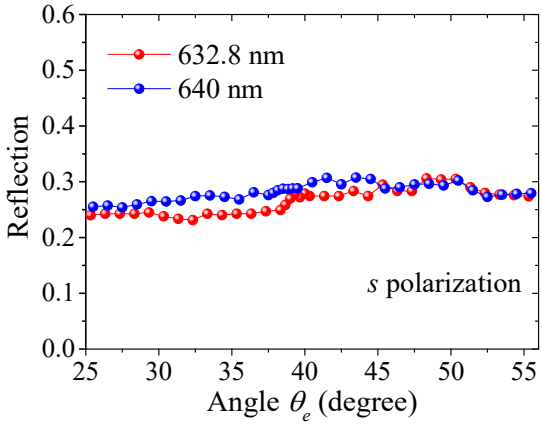

Figure S3. Experiment results of light reflection versus the incident angles θ_e in the Kretschmann configuration with a 50 nm Sb_2Te_3 film at the wavelengths of 632.8 and 640 nm for *s*-polarized incident light.

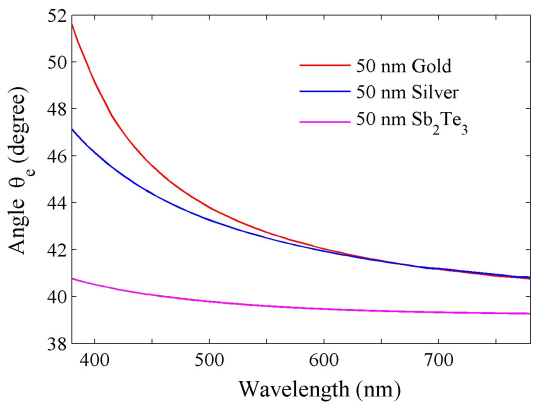

Figure S4. SPR excitation angles in the Kretschmann configurations with the 50 nm gold, silver and Sb_2Te_3 films. The dielectric constants of metals are described by the Drude model in Eq. (3). By fitting the experimental data, the parameters for gold can be set as ε_∞=1, ω_p=8.55 eV and γ=0.0184 eV. [3] The parameters for silver are set as ε_∞=3.7, ω_p=9.1 eV and γ=0.018 eV. [4]

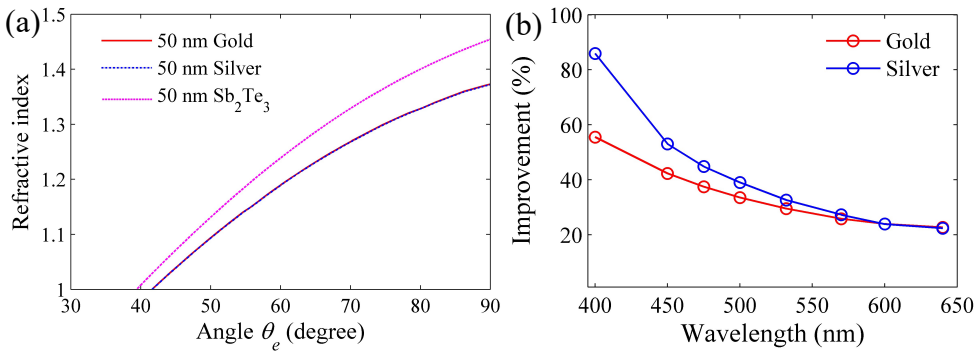

Figure S5. (a) Refractive indices of the specimen on the surface of gold, silver and Sb_2Te_3 films for the SPR excitation in Kretschmann configurations with an incident wavelength of 640 nm. The film thicknesses are set as 50 nm. Here, we can see that the maximum refractive indices for Sb_2Te_3-based and metal (gold or silver)-based SPR excitation are about 1.454 and 1.371, respectively. (b) Improvement of measurement range of refractive index for Sb_2Te_3-based SPR compared to the gold- and silver-based SPR in Kretschmann configurations at different incident wavelengths

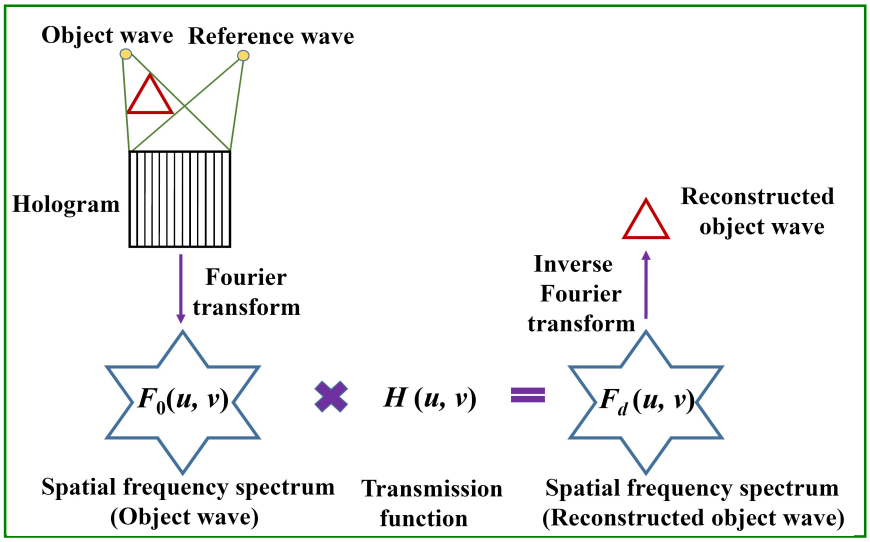

Figure S6. Processing procedure of angular spectrum reconstruction method. The light wave with object information interferes with the reference wave, generating a hologram (interference pattern). The spatial frequency spectrum $F_0(u, v)$ of the object wave is obtained from the hologram employing Fourier transform. According to the convolution method, the spatial frequency spectrum $F_d(u, v)$ of the reconstructed object wave is calculated by $F_0(u, v)\times H(u, v)$, where $H(u, v)$ stands for the transmission function. Then, we can achieve the reconstructed object wave from $F_d(u, v)$ through inverse Fourier transform.[5]

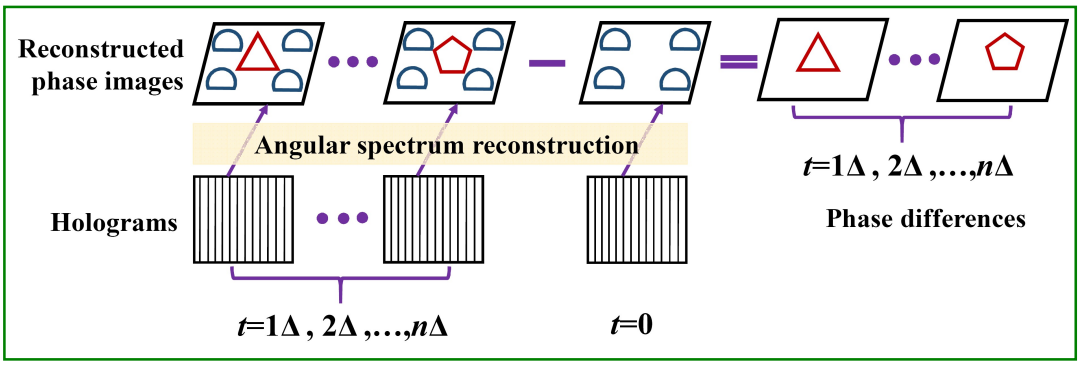

Figure S7. Double-exposure holographic interferometry for reconstructing phase differences. A background hologram (t=0) without the specimen and holograms with the specimen (t=1Δ, 2Δ,..., nΔ) are recorded to monitor a dynamic process. Δ is the time interval (e.g. Δ=3 s). The holograms are processed with angular spectrum method to reconstruct the phase images. The accurate phase differences containing the information of the specimen are obtained via subtracting the background phase image (noise) from a series of reconstructed phase images with the specimen.

Material	Ag	Au	Sb_2Te_3
Angle sensitivity	68°/RIU	37°/RIU	88.5°/RIU
Measurement range of refractive index	1-1.371	1-1.371	1-1.454

Table S1. Comparison of angle sensitivity [6] and measurement range of refractive index (λ=640 nm) between Sb_2Te_3- and metal-based SPR. We can see that the angle sensitivity of Sb_2Te_3-based SPR is about 1.3 (2.4) fold larger than that of silver (gold)-based SPR systems. The measurement range of refractive index is improved by 22.4% at the wavelength of 640 nm for the SPR based on the Sb_2Te_3 topological insulator.

References

[1] G. Jellison, Jr and F. Modine, Parameterization of the optical functions of amorphous materials in the interband region. *Appl. Phys. Lett.* 1996, **69**, 371.

[2] J. Ou, J. So, G. Adamo, A. Sulaev, L. Wang and Z. Nikolay, Ultraviolet and visible range plasmonics in the topological insulator $Bi_{1:5}Sb_{0:5}Te_{1:8}Se_{1:2}$. *Nat. Commun.* 2014, **5**, 5139.

[3] M. Blaber, M. Arnold and M. Ford, Search for the ideal plasmonic nanoshell: the effects of surface scattering and alternatives to gold and silver. *J. Phys. Chem. C* 2009,**113**, 3041.

[4] P. Johnson and R. Christy, Optical constants of the noble metals. *Phys. Rev. B* 1972, **6**, 4370.

[5] M. Kim, *Digital holographic microscopy: principles, techniques and applications*. Springer, 2011.

[6] A. Abbas, M. Linman and Q. Cheng, *Sens. Actuators B: Chem.* 2011, **156**, 169.